# RECENT PROGRESS ON RANS-BASED TRANSITION MODEL VERIFICATION

N. Hildebrand<sup>1</sup>, B. S. Venkatachari<sup>2</sup>, V. Srivastava<sup>2</sup>, and M. M. Choudhari<sup>1</sup>

- <sup>1</sup> NASA Langley Research Center, Hampton, VA, 23681
- <sup>2</sup> Analytical Mechanics Associates, Hampton, VA, 23666

nathaniel.j.hildebrand@nasa.gov

# **Abstract**

The current efforts to assess and improve the Reynolds-averaged Navier-Stokes (RANS)-coupled transition models in the NASA FUN3D and OVER-FLOW codes are summarized in this study. The first AIAA Transition Modeling Workshop and the NATO AVT-313 Transition Workshop both emphasized the need for code verification for transport equationsbased transition models as a top priority. We discuss the methods used for the model verification, the resulting grid families, the flow solutions, and other supporting information collected with at least two established NASA flow solvers, namely, FUN3D and OVER-FLOW. These results, which will be uploaded onto the NASA Turbulence Modeling Resource, should assist other members of the computational fluid dynamics (CFD) community in verifying their own implementations of various transition models, such as the Langtry-Menter (LM2009) model, the one-equation  $\gamma$  model, and Coder's amplification factor transport (AFT) model. Grid convergence is assessed using both global and local flow metrics of interest such as lift and drag as well as local skin-friction coefficients. We also explore the anisotropic unstructured metric-based adaptive mesh refinement library known as refine with the NASA FUN3D solver to determine if this capability can achieve the same accuracy as handcrafted structured grids with a significantly smaller node count and to learn the characteristics of the resulting grid distribution, especially in the vicinity of the transition zone.

# 1 Introduction

Accurate modeling of boundary-layer transition is a top research priority according to the NASA CFD Vision 2030 Study by Slotnick et al. (2014). Unlike direct numerical simulations and wall-resolved large-eddy simulations, RANS models are computationally efficient and easy to implement. A significant focus of recent work in the community has been the development of transition models that are based on a similar set of transport equations, e.g., Langtry and Menter (2009), Coder (2019), and Menter (2015). These models solve equations that are rooted in empirical correlations that determine the onset of transition and only rely on local information as opposed

to integral boundary-layer parameters. This class of transition models have been known to add value for overall CFD predictions, even for complex flow configurations (Coder 2019).

From recent workshops organized by the AIAA (https://transitionmodeling.larc.nasa.gov/workshop\_i) and NATO AVT-313 (https://web.tecnico.ulisboa.pt/ ist12278/Workshop\_AVT\_313\_2D\_cases/) discussion groups, there is a significant amount of scatter in the results computed on identical grids with various flow solvers that supposedly used the same RANS-based transition-model implementation, refer to Eca et al. (2023). The present paper is an extension and summary of earlier work by Venkatachari et al. (2022), Hildebrand et al. (2023), and Venkatachari et al. (2023). Specifically, we present the findings of detailed code verification for several mainstream transition models in the NASA flow solvers FUN3D (Anderson 2022) and OVERFLOW (Nichols and Buning 2019). The selected models are the LM2009  $\gamma$ -Re<sub> $\theta$ </sub>, model by Langtry and Menter (2009), the Coder (2019) AFT model, and the Menter (2015)  $\gamma$  model. The flow configurations include flat-plate and 2D-airfoil configurations that cover a range of different transition mechanisms, namely, natural transition due to Tollmien-Schlichting waves, separation-bubble instabilities, and bypass transition due to high-intensity freestream turbulence.

Along with RANS-based transition model verification using families of nominally structured grids, we apply the anisotropic unstructured metric-based adaptive mesh refinement library known as *refine* (Park 2008) with the NASA FUN3D solver to flow over the NLF(1)-0416 airfoil at an angle of attack equal to zero degrees. The goal of this exercise is to determine if *refine* can obtain the same level of accuracy as the structured grids with much smaller node counts for natural boundary-layer transition. It will also provide useful insights about the underlying characteristics of the resulting grid distribution in the transition zone.

# 2 Methodology

FUN3D is a suite of NASA-developed CFD simulation and design codes that can be used with a variety of mesh formats, including mixed-element un-

structured grids and structured multiblock grids with one-to-one interfaces or overset grid systems. Refer to Anderson (2022) for more details about FUN3D. It can be easily coupled with the anisotropic unstructured metric-based adaptive mesh refinement library known as *refine* (Park 2008). Another important feature of this NASA suite of codes is the discretely-exact adjoint solver that can be applied to gradient-based design or automated grid adaptation. OVERFLOW 2.3e solves the Navier-Stokes equations on structured overset grids with finite-difference schemes and is capable of both steady-state and time-accurate solutions. Refer to Nichols and Buning (2019) for more details about OVERFLOW.

Currently, the LM2009 model by Langtry and Menter (2009), the Coder (2019) AFT model, and the Menter (2015)  $\gamma$  model are implemented within FUN3D and OVERFLOW. The  $\gamma$ -Re $_{\theta_{\star}}$  transition model by Langtry and Menter (2009) consists of four different transport equations in total for the turbulent kinetic energy k, the dissipation rate  $\omega$ , the intermittency  $\gamma$ , and the critical-momentum-thickness Reynolds number  $Re_{\theta_t}$ . On the other hand, the Menter (2015)  $\gamma$  transition model entails only three total transport equations for k,  $\omega$ , and  $\gamma$ , respectively, while also being Galilean invariant. Lastly, the SA-based AFT transition model by Coder (2019), which is also Galilean invariant, solves transport equations for the kinematic eddy turbulent viscosity, the modified intermittency, and the envelope amplification factor.

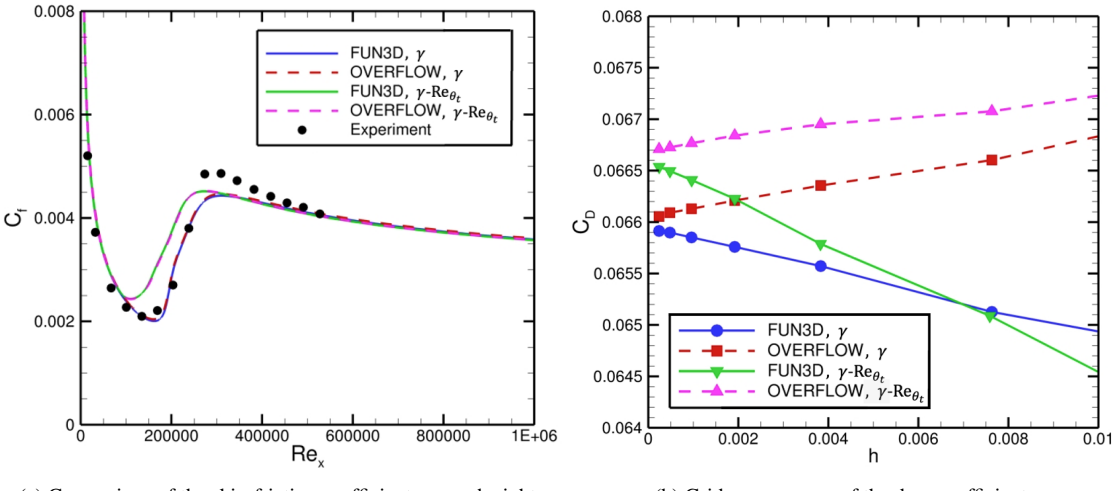
#### 3 Results

The first verification case involves the use of the  $\gamma$  and  $\gamma$ -Re $_{\theta_t}$  models for predicting bypass transition due to high freestream turbulence. Note that Coder's AFT model is not designed to predict bypass transition. We consider flow over a two-dimensional flat plate with  $M_{\infty}=0.2$ , Re  $=2\times10^5$  m<sup>-1</sup>, and  $T_{\infty}=$ 300 K. The values  $\nu_t/\nu = 11.9$  and Tu = 5.855% are specified at the inlet, which is 0.25 m upstream of the leading edge of the flat plate. Furthermore, the flatplate length is 20 m, and the top edge of the domain is 5 m from the plate. These flow conditions are based on the case labeled T3A from ERCOFTAC and the 1st AIAA Transition Modeling and Prediction Workshop. Solutions for this case are obtained without the use of any turbulence sustaining terms. The boundary conditions are wall-normal symmetry on the bottom boundary upstream of the flat-plate leading edge, an adiabatic no-slip wall after the leading edge, a Riemann characteristic top boundary, a constant-pressure outflow such that  $p/p_{\infty} = 1$ , and the subsonic inflow has a specified total pressure based on the freestream Mach number. Eight meshes are utilized for this verification case, where the number of points approximately double with each level. Mesh five has a viscous wall spacing of  $\Delta y^+ \approx 0.5$ . For more details on the computational grids, refer to Hildebrand et al. (2023) and Venkatachari et al. (2023).

Figure 1(a) displays the skin-friction coefficient distributions from the  $\gamma$  and  $\gamma$ -Re $_{\theta_t}$  transition models in FUN3D and OVERFLOW on the finest mesh level, i.e., mesh eight, along with experimental measurements from Roach and Brierley (1992). The comparisons of the skin-friction coefficients between the different NASA flow solvers show excellent agreement for both transition models. In Figure 1(a), the  $\gamma$  model provides better agreement with the experimental measurements than the  $\gamma$ -Re $_{\theta_t}$  model. Figure 1(b) shows the grid convergence of the drag coefficient from the  $\gamma$  and  $\gamma$ - $Re_{\theta_t}$  transition models in FUN3D and OVERFLOW. The grid spacing parameter is defined as  $h = 1/\sqrt{N}$ , where N is the total number of grid points. As the grid spacing parameter decreases, the drag coefficients from the FUN3D and OVERFLOW solutions converge toward one another. The drag coefficient from the  $\gamma$ -Re $_{\theta_{\star}}$  model is slightly larger than that from the  $\gamma$  model.

The next verification case we consider involves natural and separation-bubble-induced transition along the upper and lower surfaces, respectively, of the NLF(1)-0416 airfoil. This occurs at an angle of attack equal to five degrees. The flow conditions are  $M_{\infty} = 0.1$ , Re<sub>c</sub> =  $4 \times 10^6$ ,  $T_{\infty} = 300$  K,  $\nu_t/\nu = 1$ , and Tu = 0.15%. We utilize C-type meshes for this case with the farfield boundaries placed 1000 chord lengths away from the airfoil surface. Eight meshes are utilized for this verification case, where the number of points approximately double with every other level. Figure 2 shows a closeup view of mesh one for the NLF(1)-0416 airfoil. Mesh five has a viscous wall spacing of  $\Delta y^+ \approx 0.2$ . FUN3D and OVER-FLOW simulations are run with sustaining turbulence. We employ farfield Riemann invariant boundary conditions on the outer edges of the computational domain. The airfoil surface has an adiabatic no-slip wall boundary condition.

Figure 3 displays the pressure and skin-friction coefficients from the  $\gamma$  and  $\gamma$ - $Re_{\theta_t}$  transition models in FUN3D and OVERFLOW on the finest mesh level, i.e., mesh eight, along with experimental pressure coefficient measurements from Somers (1981). Comparisons of all the pressure coefficient data from the computations and experiments yield good agreement. For the separation-bubble-induced transition along the lower airfoil surface, all the skin-friction coefficient distributions agree with each other, even between the  $\gamma$  and  $\gamma$ - $Re_{\theta_t}$  models. However, for the natural boundary-layer transition along the upper airfoil surface, the  $\gamma$  and  $\gamma$ - $Re_{\theta_t}$  models result in slightly different transition locations based on the skin friction. In Figure 3(b), the agreement between the skin-friction distributions from the  $\gamma$  model in FUN3D and OVER-FLOW is excellent. Similarly, the agreement between the skin-friction distributions from the  $\gamma$ -Re $_{\theta_{\star}}$  model in FUN3D and OVERFLOW is just as good. The grid convergence of the lift and drag coefficients from the



(a) Comparison of the skin-friction coefficient on mesh eight

(b) Grid convergence of the drag coefficient

Figure 1: Comparison of the skin-friction coefficient distribution and the grid convergence of the drag coefficient from the  $\gamma$  and  $\gamma$ - $Re_{\theta_t}$  transition models in FUN3D and OVERFLOW for the T3A flat plate, adapted from Hildebrand et al. (2023) and Venkatachari et al. (2023). The experimental skin-friction data is from Roach and Brierley (1992).

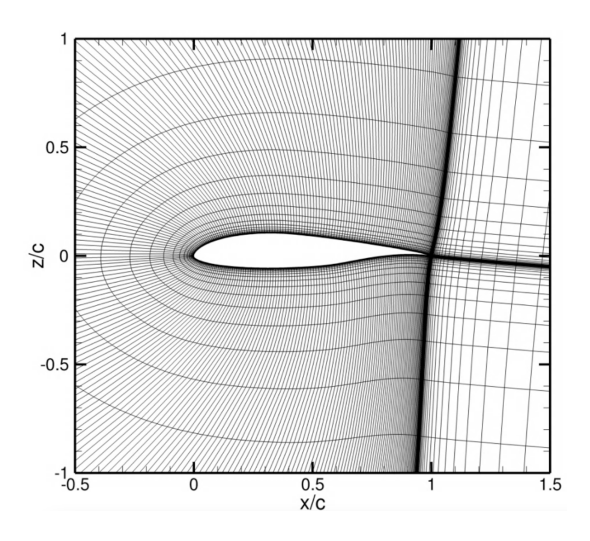


Figure 2: Closeup view of a coarse NLF(1)-0416 airfoil grid, adapted from Venkatachari et al. (2023).

the  $\gamma$  and  $\gamma$ - $Re_{\theta_t}$  transition models in FUN3D and OVERFLOW is displayed in Figure 4. Both coefficients eventually reach a nearly asymptotic state by the last two or three mesh levels for the different transition models. For the finest mesh level, there is good agreement of the lift and drag coefficients between the FUN3D and OVERFLOW implementations of the  $\gamma$  and  $\gamma$ - $Re_{\theta_t}$  models. Refer to Hildebrand et al. (2023) and Venkatachari et al. (2023) for additional comparisons of local flow metrics.

After verifying the  $\gamma$  and  $\gamma$ - $Re_{\theta_t}$  models in FUN3D and OVERFLOW for two-dimensional flow configurations, we turn our attention toward Coder's amplification factor transport model. To verify the AFT model by Coder (2019), we consider the same NLF(1)-0416 flow configuration discussed in the previous two paragraphs and Figure 2. Angles of attack

equal to zero and five degrees are considered here. Figure 5 displays the grid convergence of the skin-friction coefficient distribution in FUN3D and comparison to results with OVERFLOW on mesh level eight. For the lower surface at  $\alpha = 0^{\circ}$  and the upper surface at  $\alpha = 5^{\circ}$ , the coarser grid results in terms of the skin friction and transition locations are visibly different from the predictions based on the finest mesh level (mesh eight). However, the skin-friction distributions on mesh level eight from the FUN3D and OVER-FLOW solutions agree fairly well. Figure 6 shows a similar result in that only for mesh level eight do the lift and drag coefficients from the different NASA flow solvers agree well for the NLF(1)-0416 with  $\alpha = 5^{\circ}$ . Computations on finer grids to establish a more satisfactory grid convergence are currently in progress.

Since both FUN3D and OVERFLOW required very fine static grids to obtain accurate transition locations for two-dimensional configurations, we apply refine in conjunction with FUN3D to generate unstructured adapted grids for flow over the NLF(1)-0416 airfoil with  $\alpha = 0^{\circ}$ . The process works by starting from a baseline grid with a user-specified viscous wall spacing and initial grid complexity. The adaptive process subsequently refines the mesh based on the anisotropic metric field (i.e., Hessian of the Mach number). In the current state of development, refine does not have a transition-related metric. All results with refine have been obtained with the SA-neg turbulence model with an imposed transition location (i.e., turbulent production is switched off in the laminar regions). For the NLF(1)-0416 airfoil with  $\alpha = 0^{\circ}$ , we impose transition at  $(x/c)_{tr} = 0.41$  for the upper surface and  $(x/c)_{\rm tr}=0.52$  for the lower surface. For more details on the *refine* approach, refer to Venkatachari et al. (2022). In contrast to the adaptive mesh revisions, the static grids are refined uniformly everywhere.

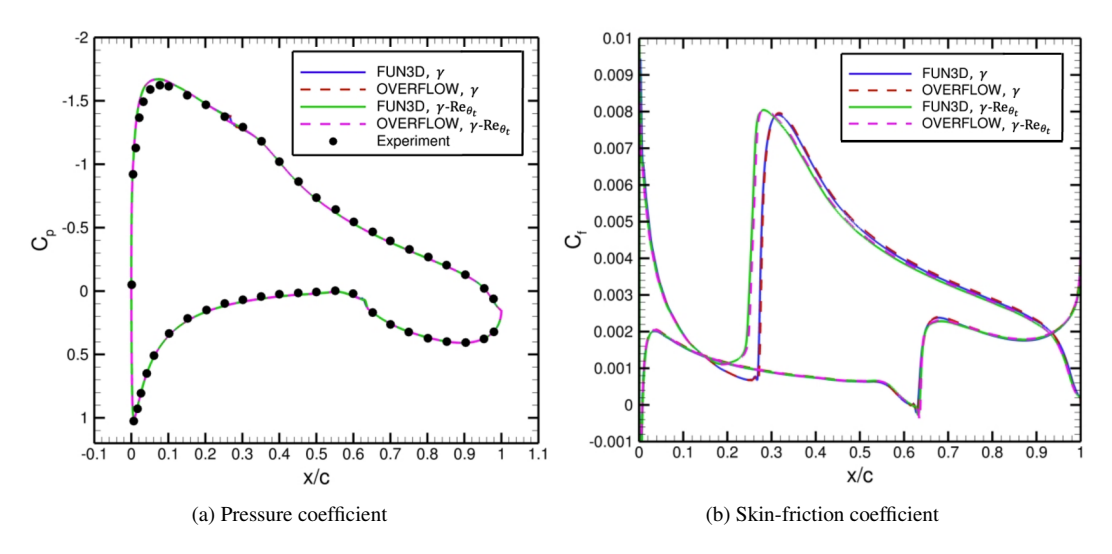


Figure 3: Comparisons of the pressure and skin-friction coefficients from the  $\gamma$  and  $\gamma$ - $Re_{\theta_t}$  transition models in FUN3D and OVERFLOW for the NLF(1)-0416 airfoil, adapted from Hildebrand et al. (2023) and Venkatachari et al. (2023). The experimental pressure coefficient data is from Somers (1981).

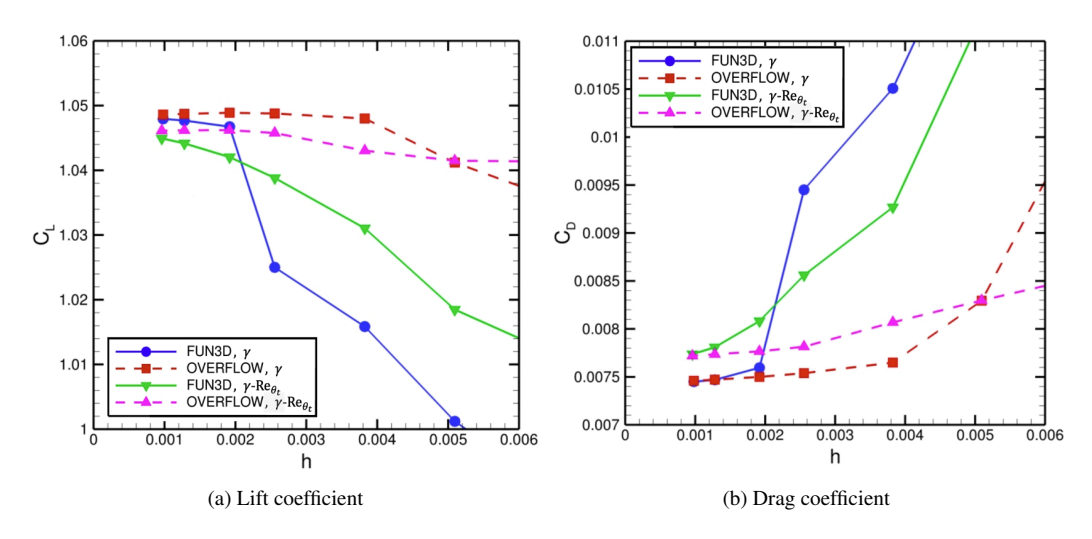


Figure 4: Grid convergence of the lift and drag coefficients from the  $\gamma$  and  $\gamma$ - $Re_{\theta_t}$  transition models in FUN3D and OVER-FLOW for the NLF(1)-0416 airfoil, adapted from Hildebrand et al. (2023) and Venkatachari et al. (2023).

Figure 7 shows the grid convergence of the pressure and skin-friction coefficient distributions for the adapted refine grids with FUN3D and comparisons to results for a fine static grid. The overall agreement of the pressure and skin-friction coefficients between adapted mesh 84 (N=2,622,426) and static mesh 8 (N = 2, 437, 825) is very good. Figure 8 displays comparisons of the lift, drag, pressure drag, and viscous drag coefficients between the static grids and adapted refine grids. We see that as the grid spacing parameter decreases, the drag, lift, and pressuredrag coefficients all converge quicker on the adapted grids (i.e., approach the converged value with less grid points/cells) than results from the static grids. This indicates that the adaptive mesh refinement efficiently resolves the inviscid coefficients. For the viscous drag coefficient in Figure 8, the trend is the reverse of that seen for the other force coefficients, with the static grid results being slightly more accurate at coarser levels than results from the adapted *refine* grids.

# 4 Conclusions

We report on a code-verification study for the Langtry-Menter  $\gamma$ - $Re_{\theta_t}$  (LM2009), Menter  $\gamma$ , and AFT2019 transition models in the NASA flow solvers FUN3D and OVERFLOW. Model verification is a critical prerequisite for model validation and the outcomes of this effort should help the CFD community with meaningful evaluation and error quantification of the existing transition models. Comparisons of the pressure, skin-friction, drag, and lift coefficients from all of the RANS-based transition models in FUN3D and OVERFLOW resulted in good agreement for the flat-plate and the NLF(1)-0416 airfoil geometries. The application of anisotropic unstructured metric-based adaptive mesh refinement with *refine* demonstrated it

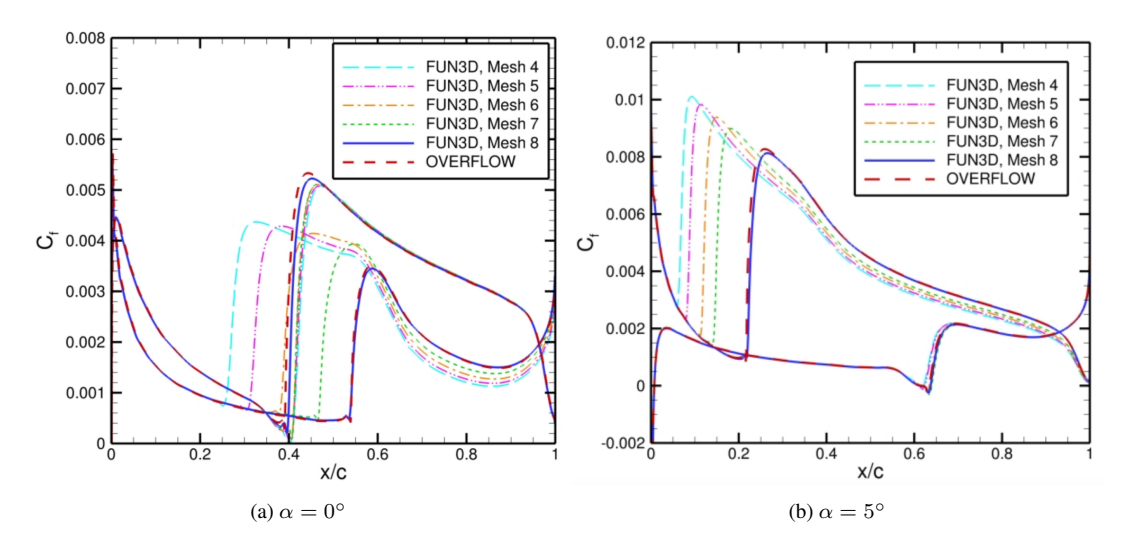


Figure 5: Grid convergence of the skin-friction coefficient distribution in FUN3D and comparison to results with OVERFLOW on mesh level eight from the AFT2019 model for the NLF(1)-0416 airfoil.

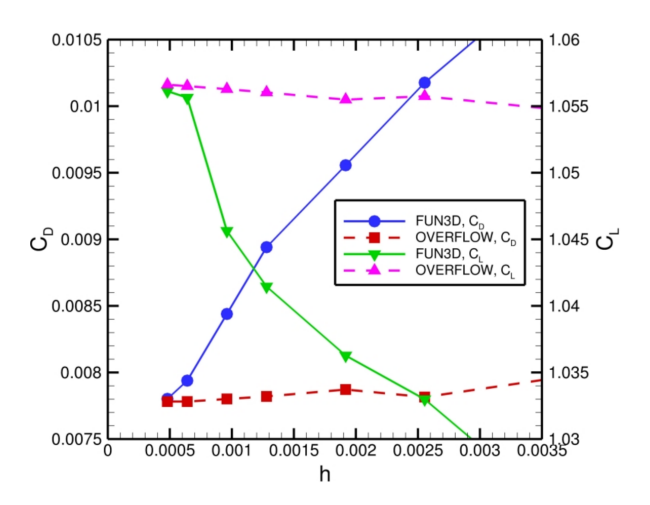


Figure 6: Grid convergence of the lift and drag coefficients from the AFT2019 model for the NLF(1)-0416 airfoil with  $\alpha=5^{\circ}$ .

can efficiently predict the force coefficients based on inviscid flow physics, but more work needs to be done so that it can efficiently resolves the viscous coefficients. Adaptive grid computations are deemed critical to facilitate model verification for complex geometries and adjoint-based solvers could play an important role in future computations of this type.

## Acknowledgments

The computations described in this paper were carried out in support of the Revolutionary Computational AeroSciences discipline under the Transformational Tools and Technologies project of the NASA Transformative Aeronautics Concepts Program.

## References

Slotnick, J., Khodahoust, A., Alonso, J., Darmofal, D., Gropp, W., and Mavriplis, D. (2014), CFD Vision 2030 Study: A Path to Revolutionary Computational AeroSciences, NASA/CR-2014-218178.

Langtry, R. B. and Menter, F. R. (2009), Correlation-Based Transition Modeling for Unstructured Parallelized Computational Fluid Dynamics Codes, *AIAA Journal*, Vol. 47, No. 12, pp. 2894–2906.

Coder, J.G. (2019), Further Development of the Amplification Factor Transport Transition Model for Aerodynamic Flows, AIAA Paper 2019-0039.

Menter, F. R. (2015), A One-Equation Local Correlation-Based Transition Model, *Flow, Turbulence, and Combustion*, Vol. 95, pp. 583-619.

Eça, L., Lopes R., Hildebrand, N., Choudhari, M. M., Rumsey, C. L., Venkatachari, B. S., et al. (2022), Assessment of Numerical and Modeling Errors of RANS based Transition Models for Low-Reynolds Numbers 2-D Flows, *Proceedings of the 34th Symposium on Naval Hydrodynamics*, pp. 1-21.

Venkatachari, B. S., Denison, M., Mysore, P. V., Hildebrand, N., and Choudhari, M. M. (2022), Toward Verification of the  $\gamma$ - $Re_{\theta_t}$  Transition Model in OVERFLOW and FUN3D, AIAA Paper 2022-3679.

Hildebrand, N., Venkatachari, B. S., and Choudhari, M. M. (2023), Implementation and Verification of the SST- $\gamma$  and SA-AFT Transition Models in FUN3D, AIAA Paper 2023-3530.

Venkatachari, B. S., Denison, M., Mysore, P. V., Hildebrand, N., and Choudhari, M. M. (2023), Verification of the  $\gamma$ - $Re\theta_t$  Transition Model in OVERFLOW and FUN3D, submitted to *Journal of Aircraft*.

Park, M. A. (2008), Anisotropic Output-Based Adaptation with Tetrahedral Cut Cells for Compressible Flows, Ph. D. Thesis, Massachusetts Institute of Technology.

Anderson, W. K., Biedron, R. T., Carlson, J.-R., Derlaga, J., Druyor, C. T., Gnoffo, P. A., Hammond, D. P., Jacobson, K.E., Jones, W. T., Kleb, B., Lee-Rausch, E. M., Nastac, G. C., Nielsen, E. J., et al. (2022), FUN3D Manual: 14.0, NASA/TM-20220017743.

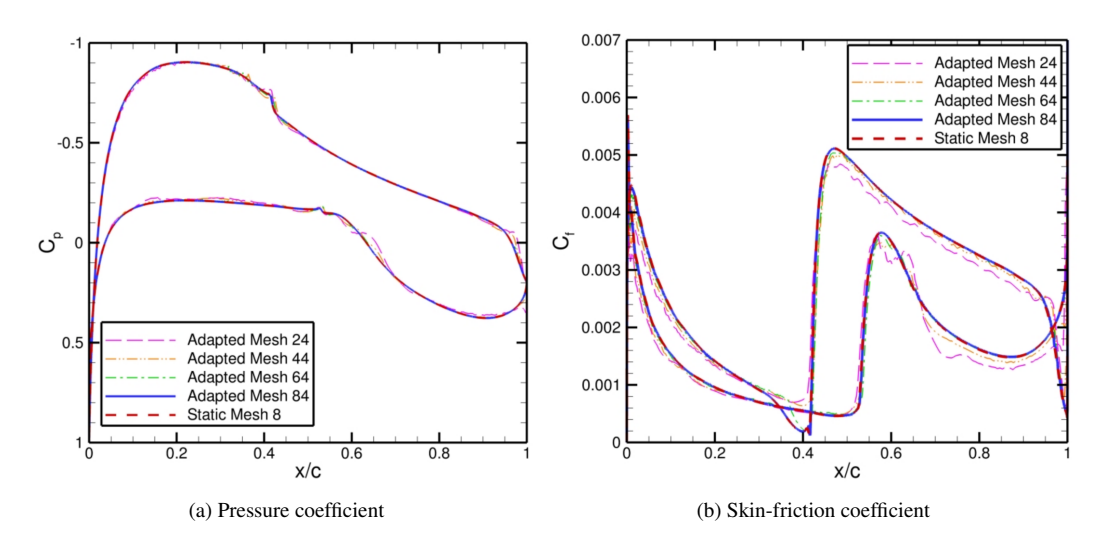


Figure 7: Grid convergence of the pressure and skin-friction coefficient distributions for the adapted *refine* grids with FUN3D and comparisons to results for a fine static workshop grid corresponding to an NLF(1)-0416 airfoil with  $\alpha=0^{\circ}$ .

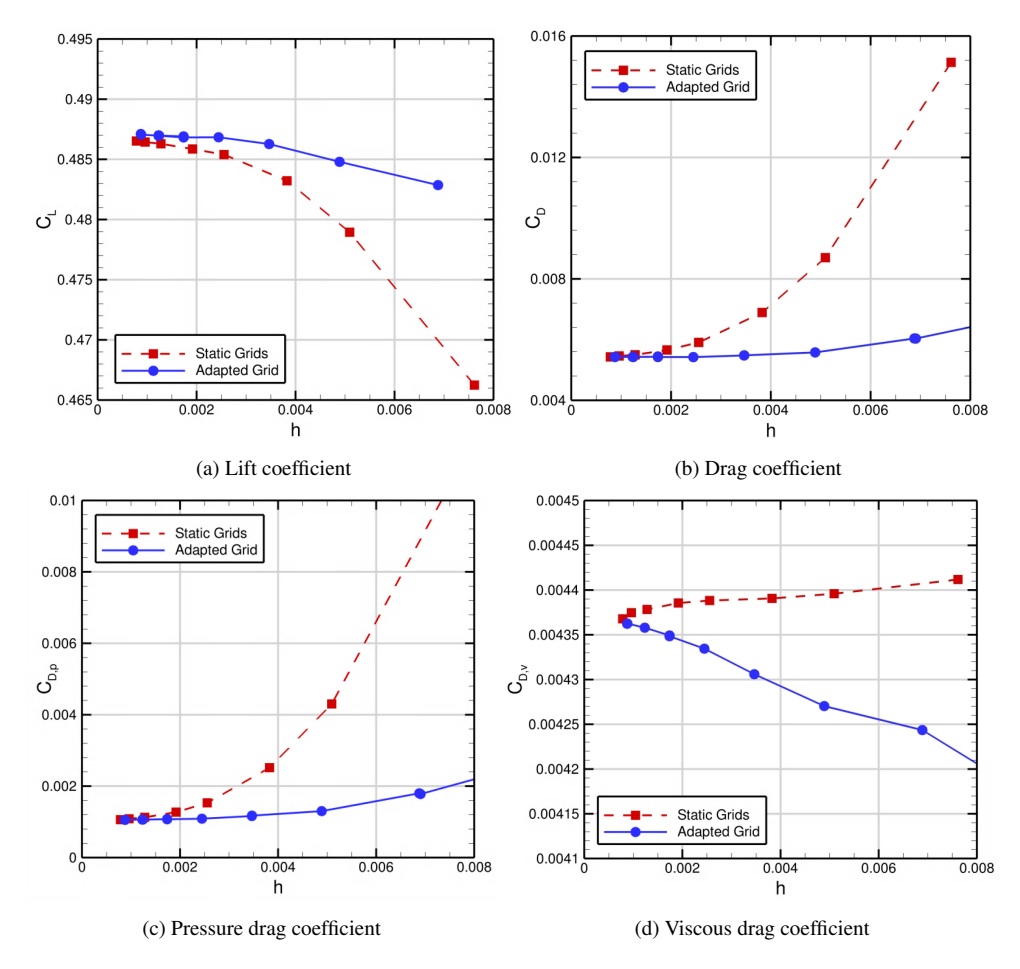


Figure 8: Comparisons of the total, pressure, and viscous drag coefficients, along with the lift coefficient, computed on static workshop grids and adapted *refine* grids with FUN3D for the NLF(1)-0416 airfoil with  $\alpha = 0^{\circ}$ .

Nichols, R. H. and Buning, P. G. (2019), User's Manual for OVERFLOW 2.3, NASA Langley Research Center, Hampton, VA.

Roach, P. E., and Brierley, D. H. (1992), The Influence of a Turbulent Free Stream on Zero Pressure Gradient Transitional Boundary Layer Development. Part 1: Test Cases T3A and T3B, *Numerical Simulation of Unsteady Flows and Transition to Turbulence*, editors O. Pironneau, W. Rodi, and I. Ryhming, Cambridge University Press, pp. 319–347.

Somers, D. M. (1981), Design and Experimental Results for a Natural Laminar Flow Airfoil for General Aviation Applications, NASA TP-1861.